



Optimization of the Photocatalytic Oxidation Process in Toluene Removal from Air

Fatemeh Khoshpasand^{1,2} | Ahmad Nikpay^{2,3✉} | Mehrdad Keshavarz^{1,2}

1. Student Research Committee, School of Health, Qazvin University of Medical Sciences, P.O.Box 34197-659811, Qazvin, Iran

2. Department of Occupational Health, School of Health, Qazvin University of Medical Sciences, P.O.Box 34197-659811, Qazvin, Iran

3. Health Products Safety Research Center, Qazvin University of Medical Sciences, P.O.Box 34197-659811, Qazvin, Iran

Article Info

Article type:
Research Article

Article history:
Received: 26 Aug 2022
Revised: 16 Nov 2022
Accepted: 14 Jan 2023

Keywords:
PCO
VOCs removal
Design of bed
RSM

ABSTRACT

The presence of volatile organic compounds in the indoor environment and their unwanted effects on human health are inevitable. That's why different methods have been proposed to remove them from air. The present study examines using photocatalytic reaction system along with TiO₂ particles coated on stainless steel webnet to study direct conversion of toluene using a new design. The study was carried out using UV radiation in a dynamic concentrator system. SEM and XRD analyses were performed to characterize prepared catalysts. Here, the aim was to employ photocatalytic oxidation (PCO) to optimize removal efficiency and elimination capacity using response surface methodology (RSM). To this end, initial concentration and flow rate were selected as independent variables. High removal efficiency and elimination capacity were realized using optimal settings. The findings indicated that PCO process with a new design other than RSM was an option to treat air pollution containing volatile organic compounds.

Cite this article: Khoshpasand, F., Nikpay, A., & Keshavarz, M. (2023). Optimization of the Photocatalytic Oxidation Process in Toluene Removal from Air. *Pollution*, 9 (2), 567-578.
<http://doi.org/10.22059/POLL.2022.347254.1595>



© The Author(s).

Publisher: University of Tehran Press.

DOI: <http://doi.org/10.22059/POLL.2022.347254.1595>

INTRODUCTION

Over the past few years, indoor air quality (IAQ) has drawn a great deal of attention in the world due to the increased amount of time people spend in indoor environments (more than 90%) (Klepeis et al., 2001; Mamaghani, Haghghat, & Lee, 2017).

Volatile organic compounds (VOCs) are an essential class of air pollutants, which considered as hazardous and generated by indoor equipment, construction material, or indoor activities like heating or cooking (Zhang, 2013). Exposure in long-term can have dire consequences for man's health (Mamaghani et al., 2017; Wang, Ang, & Tade, 2007).

The recent technologies, like non-thermal plasma (Bahri & Haghghat, 2014; Bahri, Haghghat, Rohani, & Kazemian, 2016), ozonation (Fan et al., 2003; Mamaghani et al., 2017; Zhong & Haghghat, 2014), adsorption (Haghghat et al., 2008; Shiue et al., 2010; Vizhemehr & Haghghat, 2014; Zhong, Lee, & Haghghat, 2012), and photocatalytic oxidation (Mo, Zhang, & Xu, 2013; Zhong, Haghghat, & Lee, 2013) have promised eliminating VOCs from indoor space. Photocatalytic oxidation (PCO) technology is a highly sustainable and efficient method for purifying indoor spaces. PCO technology is based on exposing a catalyst (titanium dioxide

*Corresponding Author Email: anikpey@qums.ac.ir

(TiO₂), to ultraviolet (UV) light to transform VOCs into less harmful products (Das, Rene, & Krishnan, 2018; Mamaghani et al., 2017).

The photocatalytic substrate should allow polluted air through using a low-pressure drop. High proton utilization of photocatalyst allows adequate time of contact between photocatalyst and VOC and it is (Choi, Ko, Park, & Chung, 2001; Mamaghani et al., 2017; Zhang, 2013). Numerous substrates have been proposed as a promising design to speed up the PCO process. Still, it is highly challenging due to the combined occurrence of different physical and chemical phenomena (Mohseni & Taghipour, 2004; Queffeuilou, Geron, & Schaer, 2010; Raupp, Alexiadis, Hossain, & Changrani, 2001; van Walsem, Roegiers, Modde, Lenaerts, & Denys, 2019).

The standard methods for experimenting entail several assays, which is time consuming and neglects the probable interaction between the parameters, fails to optimize the results, and it is also highly time consuming. Techniques based on statistics such as response surface methodology (RSM) has superiority compared to the limitations. Lowering the experimental errors and modeling, better optimizing and improving processes are among the advantages of RSM (Emamjomeh, Jamali, Naghdali, & Mousazadeh, 2019; Jamali & Moradnia, 2018; Khayet, Sanmartino, Essalhi, García-Payo, & Hilal, 2016).

The study mainly focused on the removal efficiency of toluene from air via the photocatalytic oxidation process using a novel design of a photocatalytic surface. Moreover, the critical factors of the PCO process, including concentration and flow rate, were optimized using the central composite design (CCD) and RSM.

MATERIALS AND METHODS

To support photocatalyst, Stainless steel webnet was used given its flexibility for engineering and also resistance to many corrossions. Moreover, the wide surface area of can enhance the active site for the deposition of TiO₂. Stainless steel webnet was designed in a folded form with middle disks to achieve higher mass and energy transfer (Fig. 1). Titanium dioxide P-25 (particle size about 25 nm; Anatase/Rutile: 80/20; and surface area: 55±15 cm²/g) was provided by the Degussa Co for coating stainless steel webnet with 0.8 mm thickness and 70 pores/in². Also, nitric acid (65%), hydrochloric acid (37%), ethanol (96%), and acetone were procured from Merck (Merajin, Sharifnia, Hosseini, & Yazdanpour, 2013; Shang, Li, & Zhu, 2003).

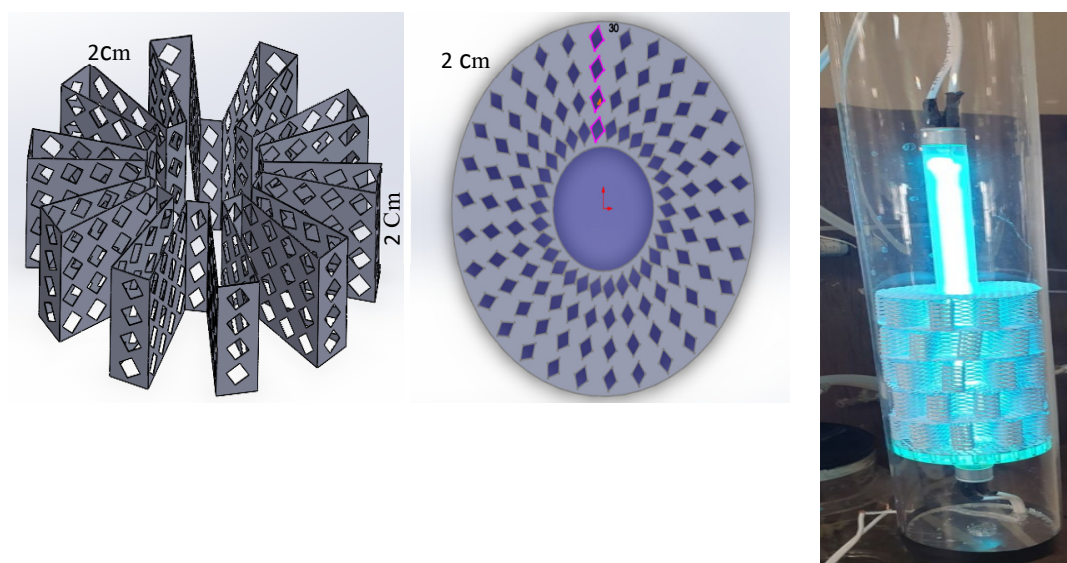


Fig. 1. Coated stainless steel webnets with titania particles

Table 1. The experimental design matrix and the operating parameters

Variables	Levels		
	-1	0	+1
A- Concentration (ppm)	10	25	40
B- Flow (L/min)	2	3.5	5

Table 2. The removal efficiencies and experimental conditions of the predicted and actual response values

std	Run	Concentration (ppm)	Flow (l/min)	RE(%)		EC(g/m ³ .min)	
				Exp.	Pred.	Exp.	Pred.
2	6	25	3.5	19	18.92	8.74	8.77
3	13	10	2	41.26	41.72	16.31	16.62
4	1	25	3.5	15.29	15.51	22.14	22.31
5	8	25	1.38	38.79	38.43	5.25	4.98
6	9	40	2	10.66	10.64	12.55	12.48
7	5	25	3.5	27.30	27.32	7.83	7.76
8	10	3.79	3.5	32.17	31.77	26.61	26.34
9	7	46.21	3.5	17.68	17.43	8.99	9.63
10	12	25	5.62	16.99	17.43	9.68	9.63
11	2	25	3.5	16.92	17.43	8.92	9.63
12	11	25	3.5	16.92	17.43	9.89	9.63
13	4	10	5	18.65	17.43	10.65	9.63

Exp: experimental; Pred: Predicted

An efficient and simple approach was proposed here to immobilize TiO₂ nanoparticles. To create titanium dioxide coating, titania slurry should be prepared using the following method. First, 2.5g of titanium dioxide powder must be mixed with 15mL ethanol to form the base medium of the slurry and then TiO₂ powder can be dispersed properly. Then, 5mL of dilute nitric acid with a pH 3.5 must be mixed to the slurry to achieve good acidity level, which is needed for the titania power to be properly dispersed. By adding the acid, the slurry gains more uniformity and the cloudiness disappears. Afterward, the slurry must be sonicated for 30min to separate the flocculated TiO₂ powder and achieve a slurry that is more uniformed. As a support, stainless steel webnet is rinsed with hydrochloric acid, distilled water, and acetone. Then, the webnet was put at room temperature for 24h to dry. Eventually, calcination is carried out in a furnace at 350°C for 30min. After completion of the coating process, the catalyst is ready (Medina-Valtierra, Moctezuma, Sánchez-Cárdenas, & Frausto-Reyes, 2005; Merajin et al., 2013; Vione et al., 2005).

A glass cylinder (21cm height and 6cm inner diameter, 339ml) was used for photocatalytic experiments with an up-flow pattern. A UV-C lamp with 8 W power (wavelength of 254 nm) was placed parallel to the airflow at a 0.5 mm distance from the center of the photoreactor (Fig. 1).

To determine the impression of factors on RE and EC efficiency, RSM based on CCD was used. The factors and the levels of coded and actual values are listed in Table 2. The factor range was determined following similar studies (Talaiekhosani, Rezaia, Kim, Sanaye, & Amani, 2021). The experiment as designed as a CCD with 13 experiments. The empirical model as showed by a 2nd order polynomial regression was employed to explain the behavior of system using Eq. (1):

$$Y = \beta_0 + \sum_{i=1}^k \beta_i x_i + \sum_{i=1}^k \beta_{ii} x_i^2 + \sum_{1 \leq i < j}^k \beta_{ij} x_i x_j + \varepsilon \quad (1)$$

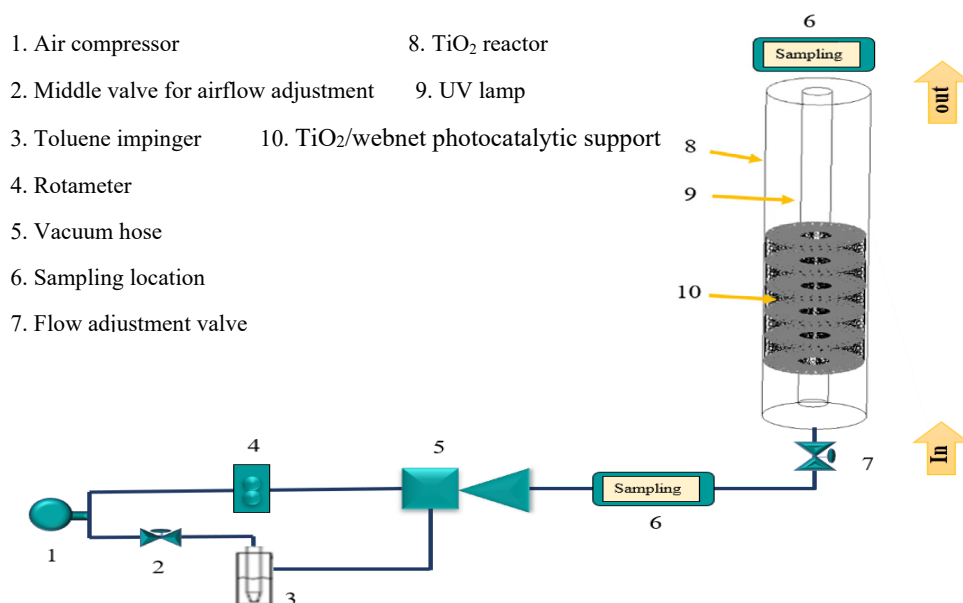


Fig. 2. Schematic of the experimental setup for the dynamic concentrator system

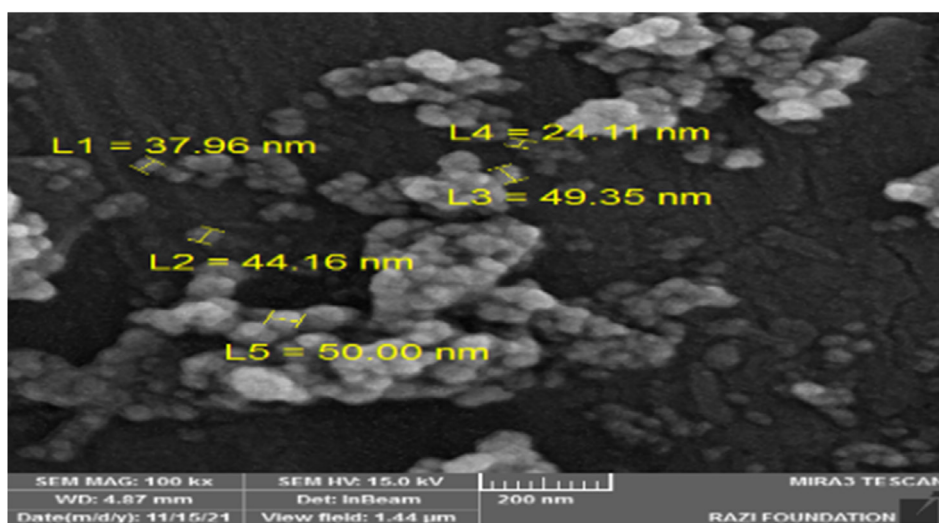


Fig. 3. The SEM image of TiO_2 surface morphology of the TiO_2 /webnet photocatalyst support

where j represents the second-order, i represents the linear constant, x_i and x_j indicate the coded independent variables, β_i is the regression constant, k refers to the investigating factors count optimized in the experiments, β_{ij} indicate the constant coefficient of reaction, ε represents the random error, and y indicates the needed responses. Table 2 lists the experimental design containing 13 randomized experiments along the five replicates of the central points.

To examine the ability of photoreduction of the prepared catalysts, toluene was converted using UV illumination at the concentration range of 10-40 ppm and airflow of 2-5 lit/min at a constant temperature. After pressure and flow adjustment and passage through a lime filter, the required airflow, supplied by a compressor, was divided into two lines for specific research purposes. At first, the system was maintained for one day in the dark before illumination to achieve the maximum toluene adsorption onto the photocatalyst surface. Then, the samples were collected from photoreactor every 30 min from the inlet and outlet of the photoreactor

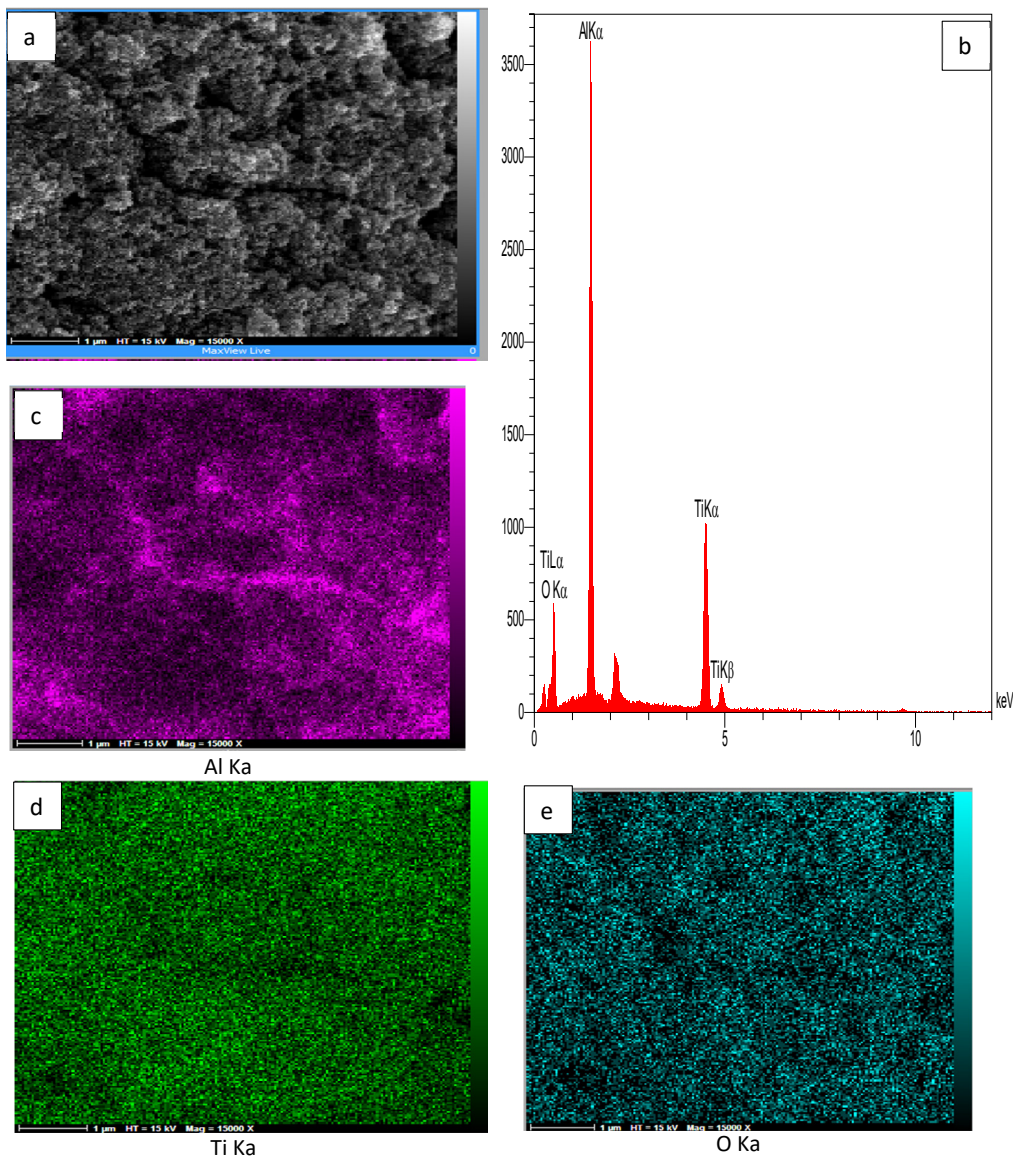


Fig. 4. The SEM image of TiO₂ calcination (a) with its EDX spectrum (b) and EDX mapping for different elements of TiO₂ composite (c-e)

with the injection of 200 μ l of gas sample to the gas chromatography model Agilent-7890B using an HP5 capillary column (30 m, 0.32 mm, 0.25 μ m) and a flame ionization detector (FID). Fig. 2 shows the schematic of the photoreactor test.

The removal efficiency and elimination capacity were calculated via Eqs. 2 and 3, respectively.

$$RE^1(\%) = \frac{C_{in} - C_{out}}{C_{in}} \times 100 \quad (2)$$

where C_{in} represents the inlet and C_{out} represents the outlet concentrations of toluene, in ppm

$$EC^2\left(\frac{g}{m^3 \cdot min}\right) = \frac{C_{in} - C_{out}}{V} \times Q \quad (3)$$

1. Removal Efficiency
2. Elimination Capacity

where C_{in} represents the inlet and C_{out} indicate the outlet concentrations of toluene, in g/m^3 , V is the reactor volume in m^3 , and Q represents the flow rate in m^3/min .

RESULTS AND DISCUSSION

Fig. 3 illustrates the morphology and scanning electron microscopy (SEM) image of the TiO_2 surface. It was observed that the distribution of nanoparticles on the webnet was similar, and the particle size in the catalyst was smaller than 50 nm and smaller than 24 nm in the absorbent catalyst. On the other hand, the size of nanoparticles let to more contact area of the pollutant with the catalyst and increases reaction and removal efficiency.

There is a need to adsorb the reactants on the surface before the photocatalytic reaction when the webnet is coated by titania particles. Based on SEM results, coatings were bonded perfectly to the webnet.

Concerning the surface property of the webnet, the wire used in the structure of the webnet has a surface that was smooth relatively. Thus, TiO_2 particles are positioned on the pores and the wires are almost free of particles.

For suitable immobilization of TiO_2 on the support and increasing its durability, the particles were calcined following the coating process on the webnet surface. The best temperature for calcination ($350\text{ }^\circ\text{C}$) was based on the previous papers with the highest activity of TiO_2

Table 3. Characteristics of the TiO_2 webnet surface

Sample ID	Thickness (μm)	Contact angle [$^\circ$]	
		Active layer (mm^2)	Support layer (nm)
TiO_2 webnet surface	20 ± 1	10 ± 0.5	15 ± 0.5

Table 4. Analysis of variance for Removal efficiency of Toluene

Source	Sum of squares	df	Mean square	F-value	P-value	
Model	1144.26	5	228.85	563.02	<0.0001	Significant
A	772.28	1	772.28	1899.96	<0.0001	
B	19.8	1	19.8	48.72	0.0002	
AB	43.03	1	43.03	105.87	<0.0001	
A^2	87.74	1	87.74	215.87	<0.0001	
B^2	255.17	1	255.17	627.78	<0.0001	
Residual	2.85	7	0.41			
Lack of fit	0.58	3	0.19	0.34	0.7978	Not significant
Pure error	2.26	4	0.57			
Cor.total	1147.11	12				
Std. dev.	0.64					
Mean	23.34					
C. V. %	2.73					
Press	7.67					
R^2	0.99					
Adjusted R^2	0.99					
Predicted R^2	0.99					
Adequate precision	71.75					

photocatalyst. Through calcination, the agglomeration declined and uniform distribution of particles decreased. Thus, the catalysts activation increased.

The high performance for the absorption of UV light by calcined photocatalysts can be attributed

to its uniform structure. Surface morphology is crucial in photocatalytic activity.

The uniform surface of calcined photocatalyst can enhance light absorption, but TiO₂ can be easily agglomerated. The uniform structures of calcined photocatalysts are shown in Fig. 4 using SEM images.

The TiO₂ webnet surface characterization is summarized in Tab. 3. The average thickness of the TiO₂ layer was 20 μ.

Elemental mapping also confirmed the formation of TiO₂ photocatalyst (Fig. 4). The dense and uniform distribution of Ti and O elements in the composite is evident. Thus, this method was successful in synthesizing the samples.

The obtained equations as coded factors are as follows for toluene RE and EC as Eqs. 4 and 5, respectively.

$$\text{Removal efficiency: } 17.43 - 9.83A + 1.57B - 3.28AB + 3.55A^2 + 6.06B^2 \quad (4)$$

$$\text{Elimination capacity: } 9.63 + 2.66A + 6.57B + 0.2AB - 0.45A^2 + 3.71B^2 \quad (5)$$

The results of analysis of variance (ANOVA) for the obtained results are listed in Tables 4 and 5. The variables of the model are given in the equation and the interactions. As shown by ANOVA results, the models is highly significant and has a low probability values. This means that the p-value was below 0.0001 for RE and EC. As indicated in these tables, the significance of all variables except for the model term of AB (EC) was confirmed 95% confidence level. The square of the correlation coefficient of the responses was determined as the coefficient of determination (R²). The value of changes in the predicted and observed responses is given by R².

Table 5. Analysis of variance for Elimination capacity of Toluene

Source	Sum of squares	df	Mean square	F-value	P-value	
Model	503.76	5	100.75	303.11	<0.0001	Significant
A	56.16	1	56.16	168.95	<0.0001	
B	345.41	1	345.41	1039.15	<0.0001	
AB	0.16	1	0.16	0.47	0.5163	
A ²	1.39	1	1.39	4.19	0.08	
B ²	95.89	1	95.89	288.49	<0.0001	
Residual	2.33	7	0.33			
Lack of fit	0.3	3	0.1	0.2	0.8919	Not significant
Pure error	2.02	4	0.51			
Cor.total	506.08	12				
Std. dev.	0.58					
Mean	11.64					
C. V. %	4.95					
Press	5.31					
R ²	0.99					
Adjusted R ²	0.99					
Predicted R ²	0.96					
Adequate precision	57.38					

That is, R^2 gives the goodness of fit of the model.

Given that the predictors count was taken into account in determining the adjusted R-squared ($Adj.R^2$), commonly $Adj.R^2$ was used to make a comparison of the model using diverse predictors. The R^2 values were achieved to be 99% for both RE and EC models. An R^2 value of 99% indicated that only 1% of variations in the obtained results for RE and EC can be used for developing models. Therefore, the coefficient indicates that regression models of the two responses are significant at 95% level of confidence. To test the adequate precision (AP) the lack of fit F -test was used.

In the case of two models, lack of fit F -test was insignificant (P -value < 0.05). AP determines the domain in the predicted response in comparison with the associated error. That is, it is the ratio of signal to noise and values above 4 are considered desirable. The values of AP for RE and EC were 71.75 and 57.38, respectively, which were all at the optimum level. In addition, low coefficient of variation (CV) represent the precise data and reliability of the experiments so that values below 10% are considered as desirable (Naghdali, Sahebi, Mousazadeh, & Jamali, 2020). CV values for RE and EC were 2.73% and 4.95%, respectively, which were all acceptable.

The degradation efficiencies of photolysis were measured within one day with catalyst and without any UV illumination. The removed toluene onto the catalysts was not observed during the dark experiment.

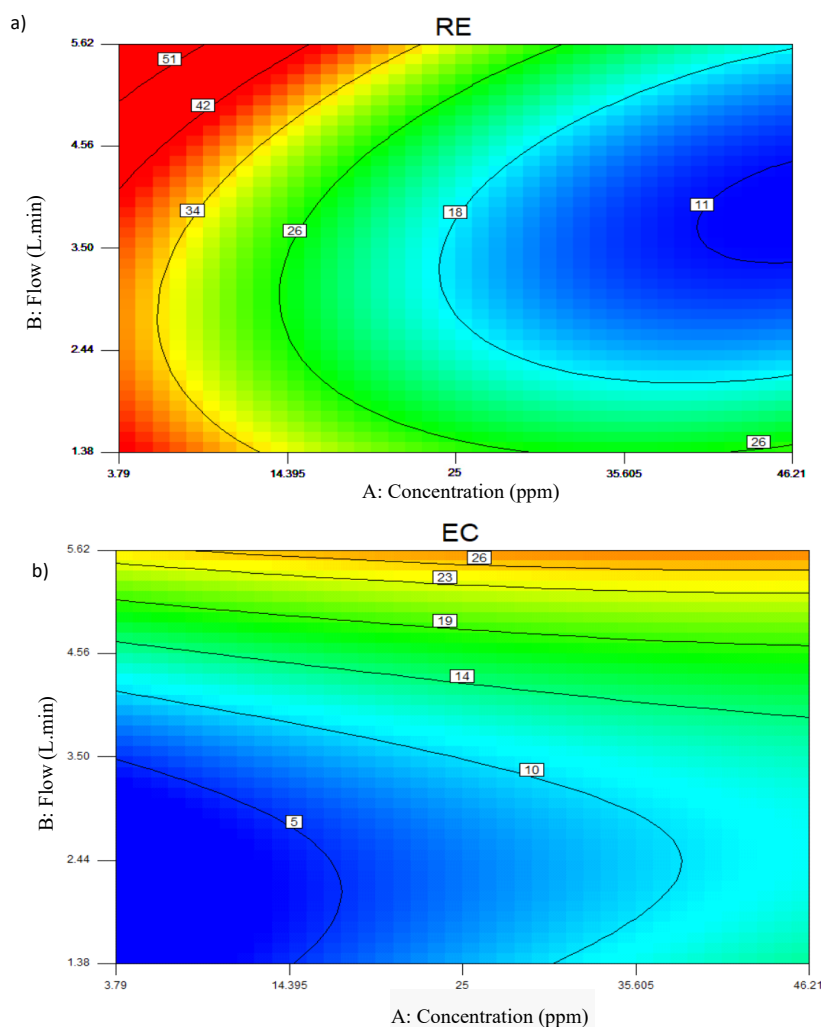


Fig. 5. Response surface plots of (a) RE(%) (b) EC($\frac{g}{m^3 \cdot min}$) and as a function of concentration and flow

Table 6. Optimum condition experiments for verification

Conditions	Responses	
	Removal efficiency (%)	Elimination capacity (g/m ³ .min)
flow= 5.61 l/min	Concentration=3.75ppm	
Actual value	58.4	24.7
Predicted value	59	25
Error	0.6	0.3
Standard deviation	±0.35	±0.2

The concentration and flow effects on the photocatalytic degradation efficiency, ranging between 3.79-6.21 ppm and 1.38-5.62 l/min of toluene, are depicted in Fig. 5a. RE is at a maximum level by increasing flow and decreasing concentration. At the fixed flow, with increasing concentration, the removal efficiency decreased for restriction active sites of TiO₂. It can be seen that the turbulent flow increases the mass transfer of the contaminants to the catalyst surface and leads to an enhancement in the effectiveness of photocatalysis. The residence time of the air contaminants is reduced. Fig. 5a illustrates that the RE rose gradually by decreasing the concentration and that the concentration effect on RE was about nine times of flow in all situations (RE= - 9.83A, 1.57B).

Liang et al. reported that the efficiency of concentration on RE was affected by a higher inlet toluene concentration and that the removal efficiency decreased from 85% to 30% (Liang, Li, & He, 2012). Moreover, Vildozo et al. indicated that the photocatalytic removal (TiO₂) of 2-propanol, with increasing the flow rate from 100 to 300 ml/min result in removal efficiency from 74% to 80% (Vildozo, Ferronato, Sleiman, & Chovelon, 2010). Also, many studies reported that RE was affected by concentration (Rezaei et al., 2007; Tanha, Rangkooy, Jaafarzadeh, Valipour, & Arefian, 2017).

The removal rate of toluene increased slowly with a higher increasing initial concentration (Fig. 5b). An explanation can be stoichiometric reaction if toluene and the active sites of TiO₂. With fixed concentration, with increasing flow, the reaction rate increased. With low concentrations, a fewer molecules are available to interact with active sites of the catalyst surface. As the initial concentration of toluene increases, the number of toluene molecules and degradation products accumulated on the photocatalyst surface increases. Therefore, a competition for adsorption happens on available active site. This inhibits the photocatalytic activity of TiO₂, which results in a decrease of hydroxyl radicals. Therefore, the efficiency of degradation efficiency of toluene decreases. In a same study, Assadi Aymen et al with assess results of the individual photocatalytic elimination capacity of emitted gases (TMA, Buty and Isoval) was determined with raise concentration (mmol/Nm³) from 0.3 to 2.7, elimination capacity increased from 5 to 25 (mg/h) (Assadi et al., 2018). In other study from Aymen Amine Assadi et al, with investigation effective of flow rate on UV/TiO₂ photocatalysis was determined the flowrate rises (four times) result in the elimination capacity rises too (from 0.14 to 0.38 g/h.m²) (Assadi, Bouzaza, Wolbert, & Petit, 2014).

Fig. 5b demonstrates that the effect of flow on EC was about 2.47 times that on the concentration, and with increasing concentration and flow rate, the elimination capacity increased (+ 2.66A + 6.57B).

According to the CCD, Table 6 lists the best condition for operation for responses (RE and EC) using the photocatalytic oxidation (PCO) process, which are Flow 5.61 l/min, Concentration=3.75ppm. The best predicted values for RE and EC were achieved to be 59%

and 25 g/m³.min, respectively. Therefore, few experiments was carried out using the optimum conditions to check the final values of the responses, which were 58.4% and 24.7 g/m³.min, respectively.

CONCLUSION

In summary, the direct conversion of toluene was conducted with nano TiO₂ particles coated on stainless steel webnet. The webnet structure allowed us to achieve a larger surface area to support TiO₂ films and increase exposure to UV light. As shown by the photocatalytic experiments, the film demonstrated a higher photocatalytic activity for the degradation of toluene photocatalytically. As shown by the SEM results, there was a perfect coating of TiO₂ on supports. In addition, the results of XRD did not indicated a significant change in the structure of photocatalysts due to the coating and calcination processes. The critical parameters of the PCO process, namely, concentration (10-40 ppm) and flow rate (2-5 l/min), were optimized for removal efficiency and elimination capacity through a CCD-RSM. With the best operational conditions (flow rate=5.61 l/min, concentration=3.75ppm), RE and EC were predicted to be 59% and 25 g/m³.min, respectively; in addition, the experiment results under the optimum conditions were 58.4% and 24.7 g/m³.min, respectively. Given the ANOVA results, R² value of the regression model equation was high and the accuracy of quadratic model was confirmed compared to the experimental data.

GRANT SUPPORT DETAILS

This paper is based on a research project under the code of 14004340 (IR.QUMS.REC.1399.056). the study was supported by the Qazvin University of Medical Sciences by funding the study. The authors also expressed their gratitude to the university for the technical support with the experimental works.

CONFLICT OF INTEREST

The authors declare that there is not any conflict of interests regarding the publication of this manuscript. In addition, the ethical issues, including plagiarism, informed consent, misconduct, data fabrication and/ or falsification, double publication and/or submission, and redundancy has been completely observed by the authors.

LIFE SCIENCE REPORTING

No life science threat was practiced in this research.

REFERENCES

- Assadi, A. A., Bouzaza, A., Wolbert, D. and Petit, P. (2014). Isovaleraldehyde elimination by UV/TiO₂ photocatalysis: comparative study of the process at different reactors configurations and scales. *Environmental Science and Pollution Research*, 21(19), 11178-11188.
- Assadi, A. A., Loganathan, S., Tri, P. N., Gharib-Abou Ghaida, S., Bouzaza, A., Tuan, A. N. and Wolbert, D. (2018). Pilot scale degradation of mono and multi volatile organic compounds by surface discharge plasma/TiO₂ reactor: investigation of competition and synergism. *Journal of hazardous materials*, 357, 305-313.
- Bahri, M. and Haghghat, F. (2014). Plasma-B used Indoor Air Cleaning Technologies: The State of the Art-R review. *CLEAN-Soil, Air, Water*, 42(12), 1667-1680.
- Bahri, M., Haghghat, F., Rohani, S. and Kazemian, H. (2016). Impact of design parameters on the

- performance of non-thermal plasma air purification system. *Chemical Engineering Journal*, 302, 204-212.
- Choi, W., Ko, J. Y., Park, H. and Chung, J. S. (2001). Investigation on TiO₂-coated optical fibers for gas-phase photocatalytic oxidation of acetone. *Applied Catalysis B: Environmental*, 31(3), 209-220.
- Das, J., Rene, E. R. and Krishnan, J. (2018). Photocatalytic degradation of volatile pollutants. *J Environ Chem Toxicol Vol*, 2(2).
- Emamjomeh, M. M., Jamali, H. A., Naghdali, Z. and Mousazadeh, M. (2019). Carwash wastewater treatment by the application of an environmentally friendly hybrid system: an experimental design approach. *Desalination and water treatment*, 160, 171-177.
- Fan, Z., Lioy, P., Weschler, C., Fiedler, N., Kipen, H. and Zhang, J. (2003). Ozone-initiated reactions with mixtures of volatile organic compounds under simulated indoor conditions. *Environmental Science & Technology*, 37(9), 1811-1821.
- Haghighat, F., Lee, C.-S., Pant, B., Bolourani, G., Lakdawala, N. and Bastani, A. (2008). Evaluation of various activated carbons for air cleaning—Towards design of immune and sustainable buildings. *Atmospheric environment*, 42(35), 8176-8184.
- Jamali, H. A. and Moradnia, M. (2018). Optimizing functions of coagulants in treatment of wastewater from metalworking fluids: prediction by RSM method. *Environmental Health Engineering and Management*, 5(1), 15-21.
- Khayet, M., Sanmartino, J., Essalhi, M., García-Payo, M. and Hilal, N. (2016). Modeling and optimization of a solar forward osmosis pilot plant by response surface methodology. *Solar Energy*, 137, 290-302.
- Klepeis, N. E., Nelson, W. C., Ott, W. R., Robinson, J. P., Tsang, A. M., Switzer, P., . . . Engelmann, W. H. (2001). The National Human Activity Pattern Survey (NHAPS): a resource for assessing exposure to environmental pollutants. *Journal of Exposure Science & Environmental Epidemiology*, 11(3), 231-252.
- Liang, W., Li, J. and He, H. (2012). Photo-catalytic degradation of volatile organic compounds (VOCs) over titanium dioxide thin film. *Advanced Aspects of Spectroscopy*, 12, 341-372.
- Mamaghani, A. H., Haghighat, F. and Lee, C.-S. (2017). Photocatalytic oxidation technology for indoor environment air purification: The state-of-the-art. *Applied Catalysis B: Environmental*, 203, 247-269.
- Medina-Valtierra, J., Moctezuma, E., Sánchez-Cárdenas, M. and Frausto-Reyes, C. (2005). Global photonic efficiency for phenol degradation and mineralization in heterogeneous photocatalysis. *Journal of Photochemistry and Photobiology A: Chemistry*, 174(3), 246-252.
- Merajin, M. T., Sharifnia, S., Hosseini, S. and Yazdanpour, N. (2013). Photocatalytic conversion of greenhouse gases (CO₂ and CH₄) to high value products using TiO₂ nanoparticles supported on stainless steel webnet. *Journal of the Taiwan Institute of Chemical Engineers*, 44(2), 239-246.
- Mo, J., Zhang, Y. and Xu, Q. (2013). Effect of water vapor on the by-products and decomposition rate of ppb-level toluene by photocatalytic oxidation. *Applied Catalysis B: Environmental*, 132, 212-218.
- Mohseni, M. and Taghipour, F. (2004). Experimental and CFD analysis of photocatalytic gas phase vinyl chloride (VC) oxidation. *Chemical Engineering Science*, 59(7), 1601-1609.
- Naghdali, Z., Sahebi, S., Mousazadeh, M. and Jamali, H. A. (2020). Optimization of the forward osmosis process using aquaporin membranes in chromium removal. *Chemical Engineering & Technology*, 43(2), 298-306.
- Queffeuilou, A., Geron, L. and Schaer, E. (2010). Prediction of photocatalytic air purifier apparatus performances with a CFD approach using experimentally determined kinetic parameters. *Chemical Engineering Science*, 65(18), 5067-5074.
- Raupp, G. B., Alexiadis, A., Hossain, M. M. and Changrani, R. (2001). First-principles modeling, scaling laws and design of structured photocatalytic oxidation reactors for air purification. *Catalysis Today*, 69(1-4), 41-49.
- REZAEI, A., POURTAGHI, G. H., Khavanin, A., SARAF, M. R., HAJIZADEH, E. and Valipour, F. (2007). Elimination of toluene by Application of ultraviolet irradiation on TiO₂ nano particles photocatalyst.
- Shang, J., Li, W. and Zhu, Y. (2003). Structure and photocatalytic characteristics of TiO₂ film photocatalyst coated on stainless steel webnet. *Journal of Molecular Catalysis A: Chemical*, 202(1-2), 187-195.
- Shiue, A., Kang, Y.-H., Hu, S.-C., Jou, G.-t., Lin, C.-H., Hu, M.-C. and Lin, S.-I. (2010). Vapor adsorption characteristics of toluene in an activated carbon adsorbent-loaded nonwoven fabric media for chemical filters applied to cleanrooms. *Building and environment*, 45(10), 2123-2131.
- Talaiekhosani, A., Rezanian, S., Kim, K.-H., Sanaye, R. and Amani, A. M. (2021). Recent advances in

- photocatalytic removal of organic and inorganic pollutants in air. *Journal of Cleaner Production*, 278, 123895.
- Tanha, F., Rangkooy, H., Jaafarzadeh, N., Valipour, F. and Arefian, I. (2017). A study on photocatalytic removal of Toluene from air using ZnO-SnO₂ coupled oxide immobilized on Activated Carbon. *Iran Occupational Health*, 13(6), 1-9.
- van Walsem, J., Roegiers, J., Modde, B., Lenaerts, S. and Denys, S. (2019). Proof of concept of an upscaled photocatalytic multi-tube reactor: A combined modelling and experimental study. *Chemical Engineering Journal*, 378, 122038.
- Vildoza, D., Ferronato, C., Sleiman, M. and Chovelon, J.-M. (2010). Photocatalytic treatment of indoor air: Optimization of 2-propanol removal using a response surface methodology (RSM). *Applied Catalysis B: Environmental*, 94(3-4), 303-310.
- Vione, D., Minero, C., Maurino, V., Carlotti, M. E., Picatonotto, T. and Pelizzetti, E. (2005). Degradation of phenol and benzoic acid in the presence of a TiO₂-based heterogeneous photocatalyst. *Applied Catalysis B: Environmental*, 58(1-2), 79-88.
- Vizhemehr, A. K. and Haghghat, F. (2014). Modeling of gas-phase filter model for high-and low-challenge gas concentrations. *Building and environment*, 80, 192-203.
- Wang, S., Ang, H. and Tade, M. O. (2007). Volatile organic compounds in indoor environment and photocatalytic oxidation: State of the art. *Environment international*, 33(5), 694-705.
- Zhang, Y. (2013). Modeling and design of photocatalytic reactors for air purification: University of South Florida.
- Zhong, L. and Haghghat, F. (2014). Ozonation air purification technology in HVAC applications. *Ashrae Trans*, 120(8).
- Zhong, L., Haghghat, F. and Lee, C.-S. (2013). Ultraviolet photocatalytic oxidation for indoor environment applications: Experimental validation of the model. *Building and environment*, 62, 155-166.
- Zhong, L., Lee, C.-S. and Haghghat, F. (2012). Adsorption performance of titanium dioxide (TiO₂) coated air filters for volatile organic compounds. *Journal of hazardous materials*, 243, 340-349.